Nuclear Engineering and Technology 55 (2023) 1460–1467

Contents lists available at ScienceDirect

Nuclear Engineering and Technology

journal homepage: www.elsevier.com/locate/net

Original Article

Acute oral toxicity and bioavailability of uranium and thorium in contaminated soil

Nur Shahidah Abdul Rashid [a], Wooyong Um [a, b, c, *], Ibrahim Ijang [d], Kok Siong Khoo [e], Bhupendra Kumar Singh [a, c], Nurul Syiffa Mahzan [a], Syazwani Mohd Fadzil [e], Nur Syamimi Diyana Rodzi [e], Aina Shafinas Mohamad Nasir [f]

[a] Division of Advanced Nuclear Engineering (DANE), Pohang University of Science and Technology (POSTECH), Pohang, Gyeongbuk, 790-784, Republic of Korea
[b] Division of Environmental Science and Engineering (DESE), Pohang University of Science and Technology (POSTECH), Pohang, Gyeongbuk, 790-784, Republic of Korea
[c] Nuclear Environmental Technology Institute (NETI), Pohang University of Science and Technology (POSTECH), Pohang, Gyeongbuk, 790-784, Republic of Korea
[d] Malaysian Nuclear Agency (MNA), Bangi, Selangor, 43000, Malaysia
[e] Department of Applied Physics, Faculty of Science and Technology, The National University of Malaysia (UKM), Bangi, Selangor, 43600, Malaysia
[f] Fuel Cell Institute, The National University of Malaysia (UKM), Bangi, Selangor, 43600, Malaysia

ARTICLE INFO

Article history:
Received 2 September 2022
Accepted 9 December 2022
Available online 10 December 2022

Keywords:
Incidental ingestion
Co-contamination (U and Th)
IAEA-312
Sprague Dawley rat model

ABSTRACT

A robust approach was conducted to determining the absolute oral bioavailable (f_{ab}) fractions of ^{238}U and ^{232}Th in rats exposed to contaminated soil along with their hematotoxicity and nephrotoxicity. The soil sample is the International Atomic Energy Agency-312 (IAEA-312) certified reference material, whereas blood, bones, and kidneys of *in vivo* female Sprague-Dawley (SD) rats estimate ^{238}U- and ^{232}Th-f_{ab} fractions post-exposure. We predict the bioavailable concentration (C_{ab}) and f_{ab} values of ^{238}U and ^{232}Th after acute soil ingestion. The blood ^{238}U (0.750%) and ^{232}Th (0.028%) reach their maximum f_{ab} values after 48 h. The ^{238}U (f_{ab}: 0.169–0.652%) accumulates mostly in the kidney, whereas the ^{232}Th (f_{ab}: 0.004–0.021%) accumulates primarily in the bone. Additionally, ^{238}U is more bioavailable than ^{232}Th. Post 48 h acute ingestion demonstrates noticeable histopathological and hematological alterations, implying that intake of ^{238}U in co-contaminated soil can lead to erythrocytes and proximal tubules damage, whereas, ^{232}Th intake can harm erythrocytes. Our study provides new directions for future research into the health implications of acute oral exposures to ^{238}U and ^{232}Th in co-contaminated soils. The findings offer significant insight into the utilization of *in vivo* SD rat testing to estimate ^{238}U and ^{232}Th bioavailability and toxicity in exposure assessment.

1. Introduction

Uranium (U), thorium (Th), and their decay series are naturally occurring radioactive materials (NORM) [1]. Nevertheless, human activities, such as mining and enrichment of U or Th, agriculture activities, nuclear energy production, decommissioning of nuclear reactors, and presumably, nuclear disturbances, including the Chernobyl and Fukushima Daiichi incidents, could elevate the concentrations of U and Th in soils [1–4].

Elevated U or Th concentrations in soils induce oral exposure risk to the public and nuclear industry workers, and due to the chemical and radiological toxicity, the radionuclides are hazardous to human health [5]. Accordingly, exposure evaluation to quantify the oral intake of U and Th in contaminated media is significant and necessary for human health risk assessment. As noted by Ma et al. [6], progress in understanding U- and Th-induced health hazards and underlying toxicological mechanism research has been modest. Although the exact figures of U and Th in contaminated soil ingested orally by populations in related areas are uncertain, many contentious findings necessitate additional research since radiological risks and toxic chemical effects on reproduction and

* Corresponding author. Division of Advanced Nuclear Engineering (DANE), Pohang University of Science and Technology (POSTECH), Pohang, Gyeongbuk 790-784, Republic of Korea
E-mail address: wooyongum@postech.ac.kr (W. Um).

https://doi.org/10.1016/j.net.2022.12.011

development are raising concerns worldwide. Consequently, a complete understanding of the reactions to exposure contamination of radionuclides in humans is critical for developing exposure analysis and treatment for overexposure.

Compared to adults, children are more likely to ingest soil from hand-to-mouth activity unconsciously and could ingest approximately 100 mg of soil per day [7–9]. Incidental ingestion of soils containing high concentrations of U and Th has been linked with health effects, including nephrotoxic, hematotoxic, and a high risk of cancer [10,11]. Similarly, incidental ingestion of contaminated media from nuclear decommissioning or severe accidents is harmful to health, especially for young children [12,13]. Therefore, the present study focused on the effects of ingesting contaminated media on children, who are more vulnerable and are more often in contact with soil than adults.

In comparison to their radiotoxicity, the chemotoxicity of U and Th, which is a key concern of environmental exposure, remains understudied [6,10,11]. The notion of whether U and Th influence blood alteration is still being discussed; some studies demonstrate alteration, while others show none. Previous studies have not adequately defined the health risks associated with the bioavailability and toxicity of U and Th co-contamination in soil and their interactions, particularly in blood. Likewise, due to limited studies, the actual bioavailability of U and Th in humans post-oral ingestion remains uncertain. Accurate risk assessments are required for proper contaminated site remediation, and site-specific *in vivo* bioavailability is applicable and essential in such assessments. *In vivo* determinations of metal bioavailability in animal models are more precise than other available methods. Therefore, animal-based absolute bioavailability (f_{ab}) analysis is necessary to offer realistic health risk estimates.

The current study used an *in vivo* rat assay to assess potential health hazards brought on by acute ingestion of uranium-238 (^{238}U) and thorium-232 (^{232}Th) in co-contaminated soil. Generally, ^{238}U and ^{232}Th comprise over 99% of U and Th found in nature [1]. The investigation utilized the International Atomic Energy Agency (IAEA)-312 certified reference material (CRM) as the medium to represent U and Th contaminated soils [14]. The IAEA-312 was employed as it contains traceable amounts of naturally occurring radionuclides (U, Th, and radium-226 (^{226}Ra)) for ultimate comparison purposes. The CRM is an easily accessible homogenous soil matrix employed for accuracy and compatibility assurance in the study. The absolute ^{238}U- and ^{232}Th-bioavailability (^{238}U- and ^{232}Th-f_{ab}) were determined by employing *in vivo* Sprague-Dawley (SD) rats. Additionally, the deleterious impacts of ^{238}U and ^{232}Th post-acute ingestion were assessed, particularly hematologic and nephrological changes in SD rats. This study might be the first to use *in vivo* SD rat models to determine the ^{238}U- and ^{232}Th-f_{ab} in IAEA-312, as well as their toxicity. Future study and risk assessment initiatives involving environmental and/or contaminated soil samples, such as U and Th mining areas, nuclear power plant decommissioning, and other industrial operations, might benefit from the findings.

2. Materials and methods

2.1. Materials

The present research applied analytical grade chemicals without further purification and utilized deionized water (DIW) as the general solvent. The IAEA-312 was a CRM acquired from the IAEA in Vienna, Austria, containing U, Th, and ^{226}Ra [14]. The soil was air-dried and filtered through a $\leq$75 μm sieve. The CRM was subjected to physicochemical characterization, bioavailability, and toxicity assessments as the smaller particles could easily disseminate and trigger a worst-case scenario of incidental ingestion exposure.

2.2. Physico-chemical characterization of IAEA-312

The total concentration of ^{238}U and ^{232}Th were measured with instrumental neutron activation analysis (INAA). Prior to irradiation, 0.20 ± 0.05 g of IAEA-312 was placed in a single high-purity polyethylene irradiation vial (⌀ 1 cm × 3 cm H). Subsequently, blanks, 40 samples, and 2 standard solutions (SS) were irradiated simultaneously by employing a 4.10×10^{12} n cm^{-2} s^{-1} thermal flux in a 750 kW PUSPATI TRIGA Mark II reactor provided by the Malaysian Nuclear Agency. A total of 40 samples were set to ensure quality assurance and quality control. The analysis was performed on a rotatory rack for 5 h.

Irradiated samples were evaluated with a calibrated high-resolution coaxial Ortec Hyper-Pure Germanium (HPGe) detector at 1.9 keV energy resolution, 25.4% relative efficiency, and 1332 keV cobalt-60 (^{60}Co) gamma (γ)-ray. The Gamma Vision software evaluated peak areas, while the INAA analysis was performed in duplicates to ensure samples were thoroughly homogenized and enabled error checking during sample preparation. The results were compared to the data on the certificate to assess the accuracy of ^{238}U and ^{232}Th concentrations in the IAEA-312 sample.

Moisture and organic contents, pH, mineral compositions, and microstructure analyses were executed as the information was not included in the IAEA-312 certificate. The American Public Health Association (APHA) 4500-H^{+}B, American Society for Testing and Materials (ASTM) D2216-19, and the International Standard Organization (ISO) procedures were applied to determine the pH, moisture content, and organic content in the sample, respectively [15–19]. The mineral phase determination was carried out by employing a D/MAX-2500/PC, Rigaku X-ray diffraction (XRD) with copper (Cu) K_{α} radiation (0.154 Å). The XRD was operated at 40 kV and 100 mA, while the 2θ-scanning range was between 10° and 90° at 1-s step time and step size $2\theta = 0.02°$.

The microstructure and elemental compositions were analyzed through field emission scanning electron microscopy with energy dispersive X-ray (FESEM-EDX) (Carl Zeiss Gemini SEM 500) under high-resolution and low charging conditions on the sample surfaces. The samples were dried at 60–70 °C and coated with a layer of platinum (100 Å) for 38 s with a sputter coater (Quorum Q150RS) in a 2×10^{-3} mbar vacuum. The Torr vacuum was utilized during imaging to avoid charging effects. The sample was subjected to a low vacuum at 20 kV accelerating voltage, between 60 and 90 mA current, and 8.2 mm working distance.

2.3. The determination of ^{238}U- and ^{232}Th-f_{ab} in SD rats through bioassay **SD rats through bioassay**

The current study was performed following the guidelines for the care and use of laboratory animals as approved by the National University of Malaysia Animal Ethics Committee (UKMAEC). Seventy-two female SD rats (aged 7–9 weeks) weighing 200 ± 10 g supplied by Primanexus (Thailand) were housed in cages (a rat per cage), kept at a constant temperature of 25 °C, 50% humidity, and a 12 h dark-light cycle. The rats were provided with dry corncobs and access to Milli-Q water (Millipore, United States of America (USA)). After a week of acclimation, each rat was placed in a plastic cage. The rats were not fed for 24 h before being exposed acutely via modified pellets intake. A 0.2 g of IAEA-312 was incorporated into the diet at a soil-to-diet ratio of one to ten since this quantity triggers the case scenario of incidental ingestion exposure from a child's hand-to-mouth activities. Next, the rats were randomly assigned into two groups. Blood samples were collected from the

Table 1
Physico-chemical properties of IAEA-312. [a]The IAEA recommended values. The results were reported with a 95% confidence level. The uncertainty represented the half-width of the 95% confidence interval.

Parameter	Certified value[a]	Present work	Method of analysis
Concentration of ^{238}U (mg kg^{-1})	16.5 (15.7–17.4)	15.8 ± 0.30 (12.6–18.1)	INAA
Concentration of ^{232}Th (mg kg^{-1})	91.4 (81.3–101)	97.9 ± 0.78 (84.4–107)	
pH		10.8 ± 0.01	APHA 4500-H + B
Moisture content (%)		2.19 ± 0.01	ASTM D2216-19
Organic content (Ca, K, N) (%)		0.35 ± 0.01, 1.21 ± 0.01, 0.17 ± 0.01	ISO 22145:2021, ISO 17319:2015, ISO 11261:1995

first group of SD rats at 6 h, 12 h, 24 h, 48 h, 120 h, 216 h, and 360 h post-exposure, while the second group had their bone, kidney, and feces samples collected at 24 h, 48 h, 120 h, 216 h, and 360 h after exposure.

The blood was collected and measured in a pre-calibrated tube containing dipotassium ethylenediamine tetraacetic acid (K_2EDTA). The bones, kidneys, and feces were placed in universal containers, and the weights were documented. The bones were crushed into fine powder for accurate dry weight evaluation. The powder was mixed vigorously and homogenized prior to utilization. The collected samples were immediately stored at −80 °C before being freeze-dried for 24 h to eliminate moisture and then analyzed with INAA. Bioavailable concentrations of ^{238}U and ^{232}Th (C_{ab}) in the collected samples were calculated according to Equation (1). The

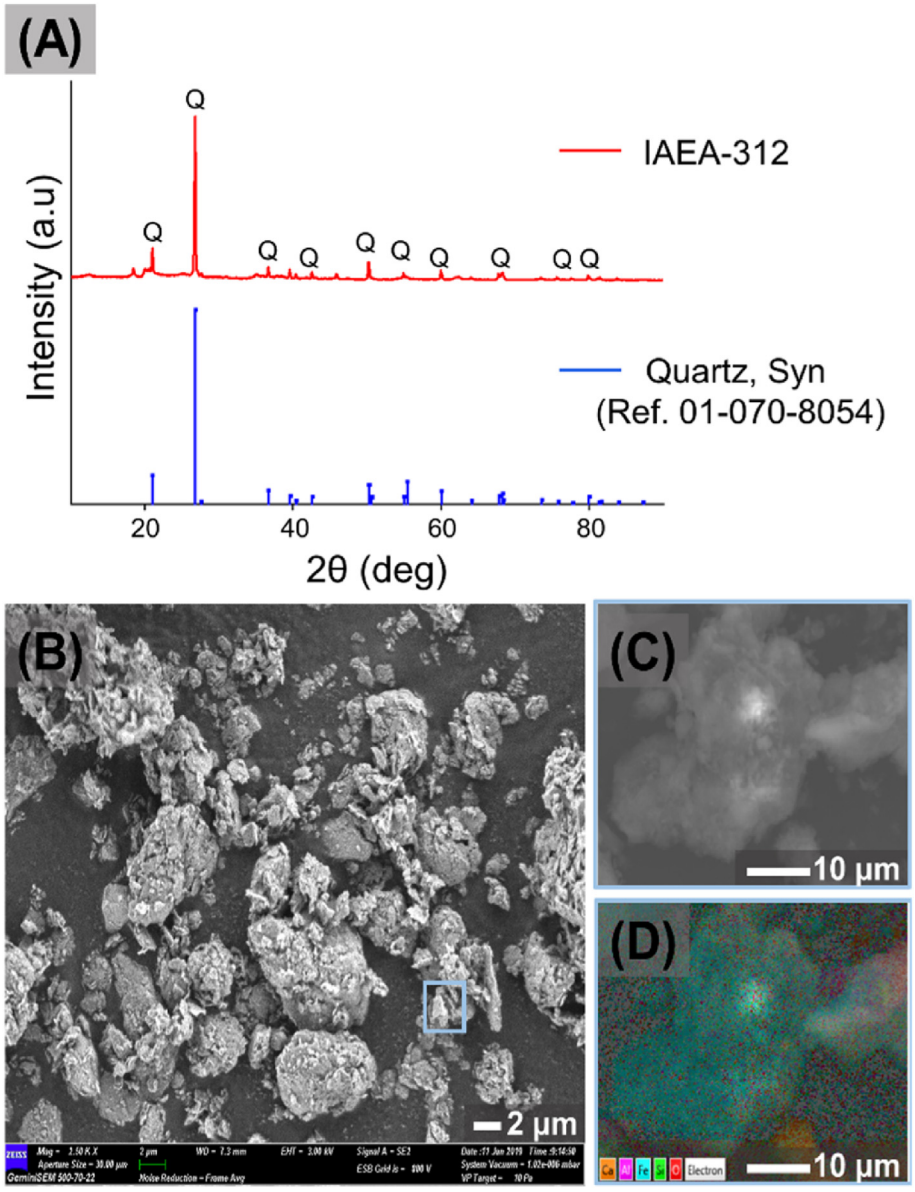

Fig. 1. Characterization results show intensity linked to quartz analysis using XRD (A), FESEM images (B), the specific site of quartz grains (C), and corresponding element mapping (D).

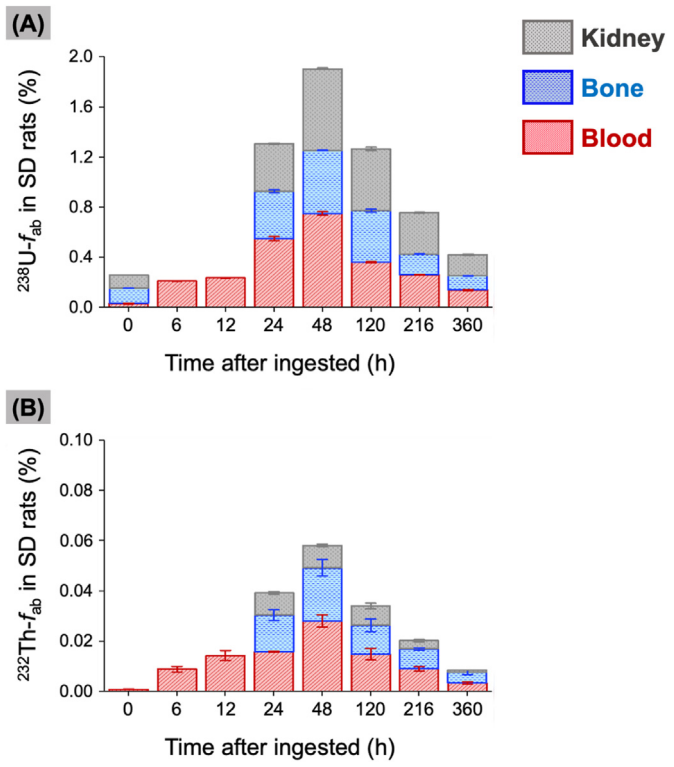

Fig. 2. The f_{ab} fractionation of ^{238}U and ^{232}Th in blood, bone, and kidney. The f_{ab} in SD rats for (A) ^{238}U and (B) ^{232}Th.

^{238}U- and ^{232}Th-f_{ab} accumulated in the blood, bone, and kidney of the SD rat was estimated based on Equation (2) [20].

$$C_{ab} = \left(\frac{A_{smp}}{A_{CRM}}\right) \times \left(\frac{W_{CRM}}{W_{smp}}\right) \times C_{CRM} \quad \text{(Eq. 1)}$$

$$f_{ab}\,(\%) = [C_{ab} \text{ in target samples}/C_{CRM}] \times 100 \quad \text{(Eq. 2)}$$

where A_{smp} and A_{CRM} are net counts of the selected peak areas in the collected samples and CRM, respectively, W_{smp} and W_{CRM} are weights of the collected samples and CRM (g), respectively, and C_{CRM} is the concentration of ^{238}U or ^{232}Th in the CRM (mg kg^{-1}).

2.4. Histopathological and hematological analyses

Histopathological and hematological analyses determined the biological effects of ^{238}U and ^{232}Th from acute ingestion at cellular levels. The sample preparations for the histopathological analysis were conducted according to the report by Almhanawi et al. [21], while the hematological evaluations were based on the study by Rahman et al. [22]. Morphological alterations in blood and kidney cells of the SD rats following ^{238}U and ^{232}Th exposure from acute ingestion were observed under a high-resolution transmission electron microscopy with energy dispersive X-ray (HRTEM-EDX) spectrometer.

The parameters measured in the hematological study included red blood cell (RBC) counts, white blood cells (WBC), and packed cell volume (PCV). In the RBC analysis, hemoglobin (Hb), and erythrocytic indices, such as mean corpuscular volume (MCV) and mean corpuscular hemoglobin concentration (MCHC), were determined. Leukocyte differential counts, including monocytes, lymphocytes, neutrophils, and platelets (PLT) were ascertained during the WBC study. The RBC, Hb, WBC, and PLT in each sample were measured with an automatic hematology analyzer (VetScan HM5, Abaxis, San Francisco, California, USA). The PCV was performed manually with microhematocrit capillary tubes.

3. Results and discussion

3.1. Characterization of IAEA-312

Table 1 summarizes the physicochemical properties of IAEA-312. The CRM is a highly alkaline soil (pH of 10.8 ± 0.01) that is low in moisture (2.19%) and organic contents (Ca = 0.35%; K = 1.21%; N = 0.17%). The experimentally determined ^{238}U and ^{232}Th concentrations were 15.7–17.4 mg kg^{-1} and 81.3–101.5 mg kg^{-1}, whereas the recommended values were 16.5 mg kg^{-1} and 91.4 mg kg^{-1}, respectively [14]. The experimental to certified concentration ratio was proportionate to the standards, where the total deviation from the certified values was 1%. Consequently, the INAA was appropriate for ^{238}U and ^{232}Th measurements and applicable for elemental analyses in biological samples, particularly for f_{ab} calculations.

The XRD results exhibited major diffraction patterns (Fig. 1A) that correlated with the reference pattern of a quartz mineral (Powder Diffraction File, Card No.: 01-070-8054 Quality: S). The data identified quartz (SiO_2) as the primary crystalline mineral in

Table 2
C_{ab} of ^{238}U and ^{232}Th in blood, bone, kidney, and feces obtained from SD rats.

Time after ingested (h)		Concentration of ^{238}U-C_{ab} (mg kg^{-1})				Concentration of ^{232}Th-C_{ab} (mg kg^{-1})			
		Blood	Bone	Kidney	Feces	Blood	Bone	Kidney	Feces
Control	**Range**	0.004–0.006	0.019–0.021	0.015–0.019	0.676–0.968	0.001–0.002	<0.0001	<0.0001	<0.0001
	GM/GSD	0.005/0.001	0.020/0.001	0.017/0.001	0.777/0.091	0.002/0.001			
6	**Range**	0.033–0.037				0.007–0.010			
	GM/GSD	0.035/0.002				0.008/0.001			
12	**Range**	0.038–0.040				0.011–0.015			
	GM/GSD	0.039/0.001				0.013/0.002			
24	**Range**	0.080–0.102	0.050–0.075	0.058–0.071	2.67–3.28	0.013–0.015	0.011–0.015	0.008–0.009	14.0–26.0
	GM/GSD	0.091/0.016	0.063/0.012	0.063/0.004	2.98/0.183	0.015/0.001	0.013/0.002	0.008/0.0006	18.3/4.71
48	**Range**	0.105–0.143	0.080–0.085	0.100–0.115	4.01–6.44	0.024–0.028	0.017–0.024	0.008–0.009	19.1–38.1
	GM/GSD	0.124/0.015	0.083/0.002	0.108/0.006	5.72/0.946	0.026/0.002	0.019/0.003	0.008/0.001	30.5/6.15
120	**Range**	0.051–0.066	0.050–0.076	0.060–0.100	4.25–6.73	0.011–0.016	0.009–0.015	0.006–0.009	19.7–39.0
	GM/GSD	0.060/0.004	0.068/0.012	0.081/0.014	5.74/0.747	0.014/0.002	0.011/0.003	0.007/0.001	30.5/5.46
216	**Range**	0.039–0.046	0.026–0.028	0.046–0.058	4.85–6.74	0.007–0.009	0.007–0.008	0.002–0.004	24.3–35.0
	GM/GSD	0.043/0.003	0.028/0.001	0.055/0.005	5.74/0.555	0.008/0.001	0.007/0.001	0.003/0.001	30.3/3.84
360	**Range**	0.017–0.029	0.017–0.020	0.021–0.039	3.50–4.92	0.002–0.004	0.003–0.006	0.001–0.002	20.2–41.5
	GM/GSD	0.023/0.005	0.019/0.001	0.028/0.006	4.28/0.415	0.003/0.001	0.004/0.001	0.002/0.001	27.3/6.74

Table 3
f_{ab} of ^{238}U and ^{232}Th in blood, bone, and kidney.

Time after ingested (h)	^{238}U (%)			^{232}Th (%)		
	Blood	Bone	Kidney	Blood	Bone	Kidney
0	0.030	0.122	0.105	0.001		
6	0.212			0.009		
12	0.237			0.014		
24	0.548	0.379	0.382	0.016	0.015	0.009
48	0.750	0.505	0.652	0.028	0.021	0.009
120	0.362	0.412	0.493	0.015	0.012	0.008
216	0.259	0.167	0.332	0.009	0.008	0.003
360	0.139	0.113	0.169	0.004	0.004	0.001

IAEA-312 with the characteristic diffraction patterns at $2\theta = 20.54$, 20.92, 26.72, and 50.21° for SiO_2.

The microstructure of the IAEA-312 samples (Fig. 1B–D) was analyzed with FESEM. Resultantly, irregular shapes and varying soil particle sizes were revealed. The FESEM micrographs at higher magnification confirmed the porous and cracking structures that influenced the soil properties. The soil composition was dominated by Si (42.7 wt %), O (21.0 wt %), Fe (16.8 wt %), Ca (8.08 wt %), K (7.88 wt %), As (3.40 wt %), and other elements (0.16 wt %).

3.2. Accumulation of ^{238}U and ^{232}Th in biological samples

In the present study, SD rats were chosen due to cost-efficiency, enabling the expansion of sample size for assays, which improved the predictive value of the obtained data. In addition, straightforward handling and extensive usage of rat-based assays in various laboratories were the reasons for selecting the SD rats. The presence of ^{238}U and ^{232}Th did not affect diet palatability and the final body weights of the SD rats, as the means did not vary (analysis of variance, $p = 0.060$).

Table 2 displays the retention of ^{238}U and ^{232}Th in blood, bone, kidney, and feces versus time following acute ingestion of IAEA-312 in female SD rats. The measured results correspond to the geometric mean (GM) of measurements obtained from six SD rats of the same age, and the uncertainties in geometric standard deviation (GSD) were below 0.1%. The control values were subtracted from each average value from the six rats.

The feces contained the highest amounts of ^{238}U (2.67–6.74 mg kg^{-1}) and ^{232}Th (14.0–41.5 mg kg^{-1}) compared to the levels determined in blood, bone, and kidney. Approximately 40–45% of ^{238}U and ^{232}Th in the fecal output suggested that ^{238}U and ^{232}Th in IAEA-312 were insoluble, hindering their absorption into the systemic circulation. Fecal elimination was sufficient to measure the net retention but not the absorption into the bloodstream. Accordingly, a sole f_{ab} determination based on established levels in the feces samples was inadequate due to severe carryover effects and co-elution of the matrix components. Correspondingly, only blood, bone, and kidney measurements were included in the f_{ab} calculation.

Other than feces samples, the C_{ab} and f_{ab} of ^{238}U and ^{232}Th values in blood, bone, and kidney samples varied significantly (Fig. 2, Tables 2 and 3), reflecting the distinct influences in the accumulation of the substances in the particular organ. Both ^{238}U- and ^{232}Th-f_{ab} in the blood (^{238}U-f_{ab}: 0.139–0.750%; ^{232}Th-f_{ab}: 0.004–0.028%) were higher than those in bone and kidney, indicating that both radionuclides were absorbed into the bloodstream before being deposited in bone and kidney. Following acute ingestion, the maximum C_{ab} and f_{ab} values of ^{238}U and ^{232}Th in the blood were reached at 48 h, respectively. Both values then declined rapidly and cleared from the systemic circulation after 48 h. Previous studies reported that the bioavailability values for U and Th were 0.002–7.00% and 0.0002–1.00%, which were absorbed into the bloodstream from the intestines [8,23–25]. The findings were

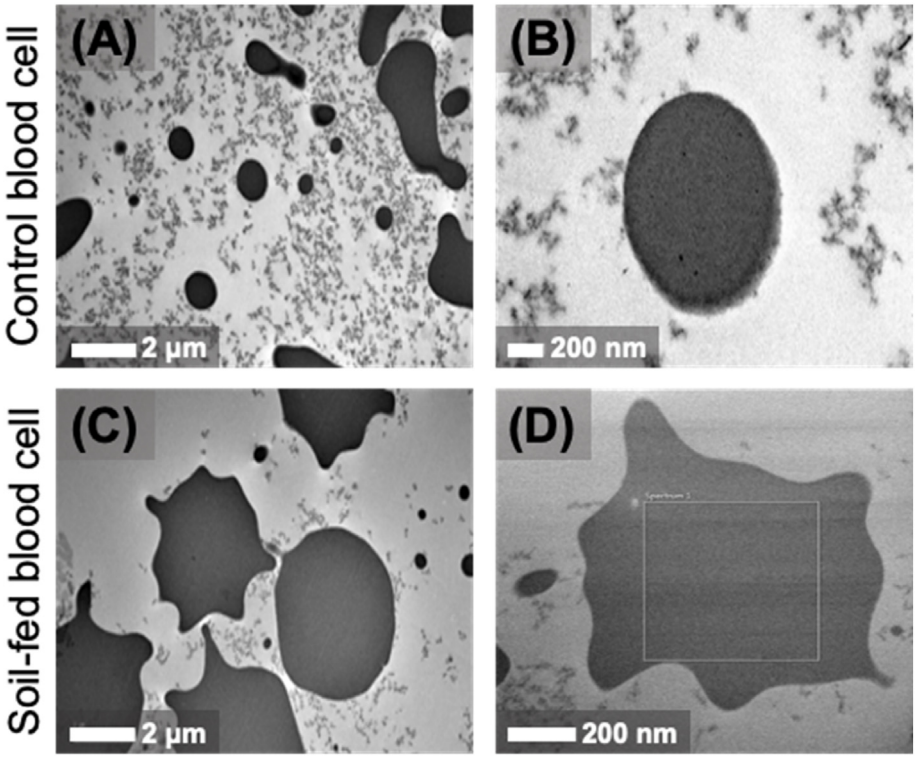

Fig. 3. The HRTEM analysis of blood cells (A–D). Comparisons between erythrocyte sections from the control and IAEA-312-treated SD rat after being soil fed at 48 h. Control erythrocytes demonstrated typical biconcave shapes, while treatment with IAEA-312 induced shape alterations and aggregation at pH 7.3–7.5.

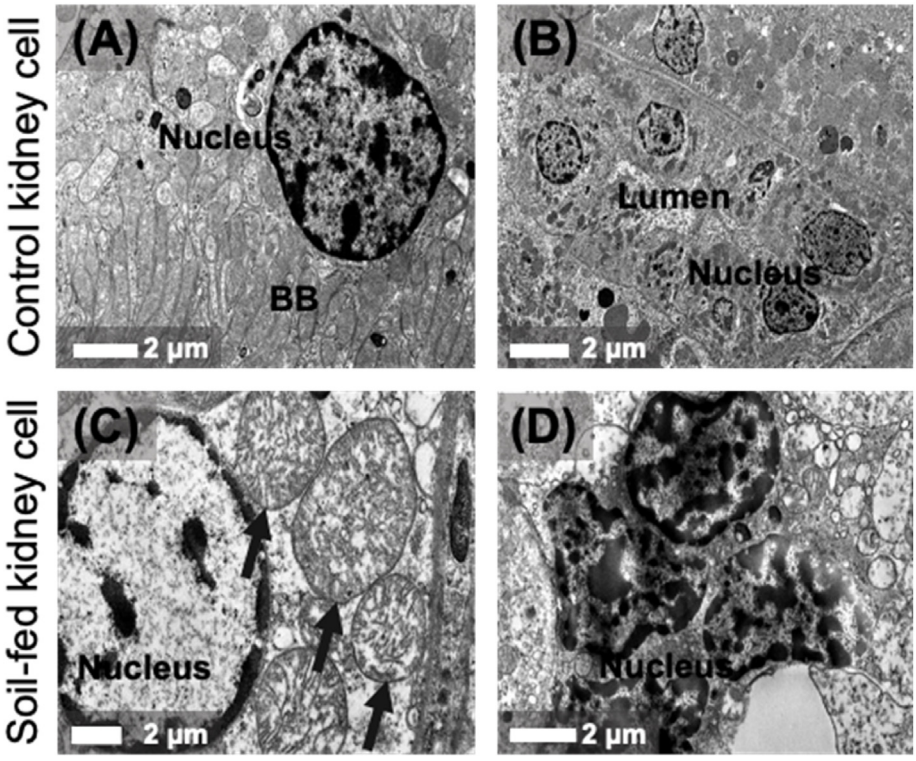

Fig. 4. The HRTEM analysis of kidney cells. (A–D) Comparisons of proximal tubule sections from the control and IAEA-312-treated SD rat after being soil fed at 48 h, (C) altered nucleus shape, and (D) mitochondrial swelling. The arrow (in Figure C) indicates a mitochondrion and BB = border brush.

Table 4
Element composition of erythrocytes and proximal tubules by EDX analysis.

Element (wt. % ± σ %)	Erythrocytes		Proximal tubules	
	Control	Treated	Control	Treated
C	51.8 ± 0.2	58.3 ± 0.3	21.3 ± 2.0	32.4 ± 2.4
Fe	16.5 ± 0.8	15.4 ± 0.7	6.8 ± 0.8	10.3 ± 0.9
O	13.3 ± 0.3	14.7 ± 0.8	5.7 ± 1.0	7.6 ± 0.7
U	<0.001	0.4 ± 0.2	<0.001	0.6 ± 0.3
Th	<0.001	0.2 ± 0.1	<0.001	<0.001

consistent with another investigation that established high values of ^{238}U- and ^{232}Th-f_{ab} in blood, ^{238}U in the kidney, and ^{232}Th in bone samples [10,11].

In the present study, the retention of ^{238}U in the kidney (f_{ab}: 0.169–0.652%) was higher than in the bone (f_{ab}: 0.113–0.505%), suggesting a potential preference accumulation of ^{238}U in the kidney. The predicted ^{232}Th-f_{ab} in bone (f_{ab}: 0.004–0.021%) was higher than in the kidney (f_{ab}: 0.001–0.009%) samples, indicating a potential preference for accumulation of ^{232}Th in the bone instead of the kidney. The high accumulation of ^{238}U and ^{232}Th in the kidney at 360 h post-acute ingestion of IAEA-312 might be due to the continuous elimination of the substances through the kidney and urine. The accumulation of ^{238}U and ^{232}Th in bone resulted from the calcification of bone and the binding of UO_2^{2+} and Th^{4+} with phosphoryl functional groups and carboxyl functional groups [26,27].

The bioavailability values obtained during the current study were considerably lower than previous works due to the soil composition differences, which greatly influenced U and Th solubility in the gastrointestinal (GI) tracts. Jovanovic et al. stated that soil samples containing a proportion of sand were hardly soluble in the simulated GI fluids, consistent with our XRD and FESEM-EDX results [28]. Quartz, being the primary mineral in IAEA-312, might be the main cause of the low bioavailability of ^{238}U and ^{232}Th.

The mechanisms of interactions between ^{238}U and ^{232}Th are

Table 5
Hematology of control and treated SD rats. Results presented as GM and GSD.

Parameters	Time after ingested (h)				
	Control	6	12	24	48
RBC (× 10^{12}/L)	8.56 ± 0.22	8.60 ± 0.14	8.57 ± 0.40	8.20 ± 0.20	7.74 ± 0.68
Hb (g/L)	163 ± 1.04	164 ± 0.45	163 ± 0.96	172 ± 1.10	177 ± 1.51
MCV (fL)	46.2 ± 0.52	46.7 ± 0.28	47.3 ± 0.21	51.0 ± 0.20	55.0 ± 1.18
PCV (L/L)	0.45 ± 0.08	0.42 ± 0.03	0.42 ± 0.07	0.40 ± 0.07	0.40 ± 0.08
MCHC (gL)	366 ± 2.92	404 ± 0.27	413 ± 0.75	428 ± 3.07	438 ± 3.98
WBC (× 10^9/L)	8.08 ± 1.25	7.87 ± 0.76	7.40 ± 0.94	9.45 ± 2.03	15.4 ± 2.57
Monocyte (× 10^9/L)	0.38 ± 0.22	0.34 ± 0.15	0.36 ± 0.19	0.55 ± 0.47	0.87 ± 0.67
Lymphocyte (× 10^9/L)	6.23 ± 1.16	5.51 ± 0.71	5.93 ± 0.83	7.95 ± 1.33	9.35 ± 1.72
Neutrophil (× 10^9/L)	1.25 ± 0.57	1.11 ± 0.23	1.15 ± 0.34	2.30 ± 0.23	4.90 ± 0.81
PLT (× 10^9/L)	1240 ± 7.70	1220 ± 3.92	1330 ± 4.12	1370 ± 8.45	1602 ± 18.1

generally uncertain. Under the applied physiological conditions, both radionuclides are stable in hexavalent (UO_2^{2+}) and tetravalent (Th^{4+}) states, forming strong complexes with biological ligands in blood or tissues [29]. The higher retention of ^{238}U compared to ^{232}Th in different biological compartments implied that the relatively high solubility of ^{238}U potentially reduced ^{232}Th in GI tracts. In the present study, the total concentration of ^{232}Th (91.4 mg kg^{-1}) in IAEA-312 was higher than that of ^{238}U. Nonetheless, ^{238}U exhibited higher solubility than ^{232}Th. The coexistence of ^{238}U led to competition between UO_2^{2+} and Th^{4+}, confirmed by Höllriegl et al. and Foulkes et al. [24,30].

3.3. The effects of ^{238}U and ^{232}Th on histopathological and hematological features of blood and kidney of the SD rats

After entering the bloodstream, ^{238}U and ^{232}Th interacted with blood components and were deposited in the kidney. After 48 h of IAEA-312 exposure, when bioavailability was at its highest, the anatomical changes in SD rats were examined using the HRTEM and EDX analyses. The anatomical changes in controlled and treated rats, especially in the erythrocytes and proximal tubules, were noticeable during the end phase. The control SD rats exhibited well-structured cellular architecture with normal, biconcave-shaped erythrocytes, and proximal tubules (Fig. 3 and Fig. 4). Upon 48 h of acute exposure to ^{238}U and ^{232}Th, shape alterations (echinocytes) and aggregation were observed in the samples. Also, found were histopathological modifications, including altered nucleus shape and swollen mitochondria within proximal tubules. The EDX spectra demonstrated the composition of U in erythrocytes and proximal tubules at 0.4 wt % ± 0.2 %–0.6 wt % ± 0.3% (Table 4). However, ^{232}Th was only detected in erythrocytes at 0.2 wt % ± 0.1%. The results confirmed that erythrocytes and proximal tubules were damaged by ^{238}U intake, while ^{232}Th intake only impairs erythrocytes. Significant hematological effects (Table 5) were established, considering that increased Hb, MCV, MCHC, WBC, monocyte, lymphocyte, neutrophil, and PLT were observed at 48 h post-acute ingestion, correlating with the maximum C_{ab} and f_{ab} values measured in SD rats. Nevertheless, RBC and PCV decreased simultaneously, indicating increased RBC damage in line with the aforementioned histopathological findings. Increased WBCs and lymphocytes in the present study were possibly from the ability of WBCs to counter inflammation due to ^{238}U and ^{232}Th ingestion.

4. Conclusion

Post-acute ingestion of IAEA-312, ^{238}U and ^{232}Th in co-contaminated soil was distributed and accumulated in blood > kidney > bone and blood > bone > kidney, respectively. Intake of ^{238}U was harmful to erythrocytes and proximal tubules, while ^{232}Th intake only impair erythrocytes. Furthermore, post-acute ingestion of ^{238}U and ^{232}Th at 48 h exhibited apparent hematological effects, significantly increased Hb, MCV, MCHC, WBC, monocyte, lymphocyte, neutrophil, and PLT, and decreased RBC and PCV. Accordingly, exposure to ^{238}U and ^{232}Th in co-contaminated soil should be controlled as future health implications will occur due to their low and long-lived α-emission activity from prolonged exposure. Thereupon, extensive studies on the interaction, transportation, metabolism, and mechanisms of ^{238}U and ^{232}Th in co-contaminated soil are required. The results would benefit future undertakings and environmental risk assessments focusing on data from contaminated soil samples.

Declaration of competing interest

The authors declare that they have no known competing financial interests or personal relationships that could have appeared to influence the work reported in this paper.

Acknowledgements

This work was supported by the Korea Hydro & Nuclear Power Co., Ltd. (KHNP) Research Fund Haeorum Alliance Nuclear Innovation Center.

References

[1] International Atomic Energy Agency, Extent of Environmental Contamination by Naturally Occurring Radioactive Material (NORM) and Technological Options for Mitigation, Technical Report Series No. 419, International Atomic Energy Agency, Vienna, 2003. https://www-pub.iaea.org/MTCD/publications/PDF/TRS419_web.pdf.
[2] International Atomic Energy Agency, Case Study on Assessment of Radiological Environmental Impact from Potential Exposure, International Atomic Energy Agency, Vienna, 2020. IAEA-TECDOC-1914, https://www-pub.iaea.org/MTCD/Publications/PDF/TE-1914_web.pdf.
[3] International Atomic Energy Agency, Implementation and Effectiveness of Actions Taken at Nuclear Power Plants Following the Fukushima Daiichi Accident, International Atomic Energy Agency, Vienna, 2020. IAEA-TECDOC-1930, https://www-pub.iaea.org/MTCD/Publications/PDF/TE-1930web.pdf.
[4] P.G. Martin, M. Louvel, S. Cipiccia, C.P. Jones, D.J. Batey, K.R. Hallam, I.A. Yang, Y. Satou, C. Rau, J.F.W. Mosselmans, D.A. Richards, Provenance of uranium particulate contained within Fukushima Daiichi nuclear power plant unit 1 ejecta material, Nat. Commun. 10 (1) (2019) 1–7.
[5] United Nations Scientific Committee on the Effects of Atomic Radiation, Sources, Effects and Risks of Ionizing Radiation. Volume II. Scientific Annex B: Effects of Radiation Exposure of Children, United Nations Scientific Committee on the Effects of Atomic Radiation, New York, 2013. https://www.unscear.org/unscear/uploads/documents/unscear-reports/UNSCEAR_2013_Report_Vol.II.pdf.
[6] M. Ma, R. Wang, L. Xu, M. Xu, S. Liu, Emerging health risks and underlying toxicological mechanisms of uranium contamination: lessons from the past two decades, Environ. Int. 145 (2020), 106107, https://doi.org/10.1016/j.envint.2020.106107.
[7] E.J. Calabrese, E. Stanek, R.C. James, S.M. Roberts, Soil ingestion: a concern for acute toxicity in children, Environ. Health Perspect. 105 (12) (1997) 1354–1358.
[8] S.C. Träber, V. Höllriegl, W.B. Li, U. Czeslik, W. Rühm, U. Oeh, B. Michalke, Estimating the absorption of soil-derived uranium in humans, Environ. Sci. Technol. 48 (24) (2014) 14721–14727.
[9] A.L. Juhasz, J. Weber, E. Smith, Impact of soil particle size and bioaccessibility on children and adult lead exposure in peri-urban contaminated soils, J. Hazard Mater. 186 (2–3) (2011) 1870–1879, https://doi.org/10.1016/j.jhazmat.2010.12.095.
[10] Agency for Toxic Substances and Disease Registry, Toxicological Profile for Uranium, Public Health Service, Atlanta, GA, 2013. https://www.atsdr.cdc.gov/toxprofiles/tp150.pdf.
[11] Agency for Toxic Substances and Disease Registry, Toxicological Profile for Thorium, Public Health Service, Atlanta, GA, 2019. https://www.atsdr.cdc.gov/ToxProfiles/tp147.pdf.
[12] S. Takahara, M. Ikegami, M. Yoneda, H. Kondo, A. Ishizaki, M. Iijima, Y. Shimada, Y. Matsui, Bioaccessibility of fukushima-accident-derived Cs in soils and the contribution of soil ingestion to radiation doses in children, Risk Anal. 37 (7) (2017) 1256–1267.
[13] M. Takagi, A. Tanaka, S.F. Nakayama, Estimation of the radiation dose via indoor dust in the ibaraki and chiba prefectures, 150–200 km south from the Fukushima Daiichi nuclear power plant, Chemosphere 236 (2019), 124778, https://doi.org/10.1016/j.chemosphere.2019.124778.
[14] V. Strachnov, V. Valkovic, R. Zeisler, R. Dekner, Report on the Intercomparison Run IAEA-312 Ra-226, International Atomic Energy Agency, Vienna, 1991. Th and U in soil, IAEA-AL-036.
[15] American Public Health Association, Standard Methods for the Examination of Water and Wastewater, 1912. https://doi/epdf/10.2105/SMWW.2882.082.
[16] American Society for Testing and Materials, Standard Test Methods for Laboratory Determination of Water (Moisture) Content of Soil and Rock by Mass, American Society for Testing and Materials, West Conshohocken, PA, 2019. ASTM D2216-19, https://www.astm.org/Standards/D2216.
[17] International Organization for Standardization, Fertilizers and Soil Conditioners-Mineral Soil Amendments-Determination of Total Calcium and Magnesium Content, 2021. ISO 22145:2021, Geneva, Switzerland.
[18] International Organization for Standardization, Fertilizers and Soil Conditioners-Determination of Water-Soluble Potassium Content-Potassium Tetraphenylborate Gravimetric Method, ISO 17319, Geneva, Switzerland,

2015.
[19] International Organization for Standardization, Soil Quality-Determination of Total Nitrogen-Modified Kjeldahl Method, 1995. ISO 11261:1995, Geneva, Switzerland.
[20] J.L. Schroder, N.T. Basta, J. Si, S.W. Casteel, T. Evans, M. Payton, In vitro gastrointestinal method to estimate relative bioavailable cadmium in contaminated soil, Environ. Sci. Technol. 37 (7) (2003) 1365–1370.
[21] B.H. Almhanawi, B. Khalid, T.A. Ibrahim, E.R.M. Tohit, A transmission electron microscopy study of anticoagulant-induced platelet vesiculation, Porto Biomed. J. 2 (1) (2017) 23–27, https://doi.org/10.1016/j.pbj.2016.11.002.
[22] H.S. Rahman, A. Rasedee, H.H. Othman, M.S. Chartrand, F. Namvar, S.K. Yeap, N. Abdul Samad, R.J. Andas, N. Muhammad Nadzri, T. Anasamy, K.B. Ng, Acute toxicity study of zerumbone-loaded nanostructured lipid carrier on BALB/c mice model, BioMed Res. Int. 2014 (2014), 563930.
[23] J. Chen, D. Lariviere, R. Timmins, K. Verdecchia, Estimation of uranium GI absorption fractions for children and adults, Radiat. Protect. Dosim. 144 (1–4) (2011) 379–383.
[24] V. Höllriegl, W.B. Li, K. Leopold, U. Gerstmann, U. Oeh, Solubility of uranium and thorium from a healing earth in synthetic gut fluids: a case study for use in dose assessments, Sci. Total Environ. 408 (23) (2010) 5794–5800, https://doi.org/10.1016/j.scitotenv.2010.08.020.
[25] S.C. Träber, W.B. Li, V. Höllriegl, K. Nebelung, B. Michalke, W. Rühm, U. Oeh, Calculation of internal dose from ingested soil-derived uranium in humans: application of a new method, Radiat, Environ. Biophys. 54 (3) (2015) 265–272.
[26] G. Rodrigues, J.D.D.T. Arruda-Neto, R.M.R. Pereira, S.R. Kleeb, L.P. Geraldo, M.C. Primi, L. Takayama, T.E. Rodrigues, G.T. Cavalcante, G.C. Genofre, R. Semmler, Uranium deposition in bones of Wistar rats associated with skeleton development, Appl. Radiat. 82 (2013) 105–110, https://doi.org/10.1016/j.apradiso.2013.07.033.
[27] G. Creff, S. Safi, J. Roques, H. Michel, A. Jeanson, P.L. Solari, C. Basset, E. Simoni, C. Vidaud, C. Den Auwer, Actinide(IV) deposits on bone: potential role of the osteopontin–thorium complex, Inorg. Chem. 55 (1) (2016) 29–36.
[28] S.V. Jovanovic, P. Pan, L. Wong, Bioaccessibility of uranium in soil samples from port hope, ontario, Canada, Environ. Sci. Technol. 46 (16) (2012) 9012–9018.
[29] E. Ansoborlo, O. Prat, P. Moisy, C. Den Auwer, P. Guilbaud, M. Carriere, B. Gouget, J. Duffield, D. Doizi, T. Vercouter, C. Moulin, Actinide speciation in relation to biological processes, Biochimie 88 (11) (2006) 1605–1618, https://doi.org/10.1016/j.biochi.2006.06.011.
[30] M. Foulkes, G. Millward, S. Henderson, W. Blake, Bioaccessibility of U, Th and Pb in solid wastes and soils from an abandoned uranium mine, J. Environ. Radioact. 173 (2017) 85–96, https://doi.org/10.1016/j.jenvrad.2016.11.030.